

Deep Reinforcement Learning-Based Mapless Crowd Navigation with Perceived Risk of the Moving Crowd for Mobile Robots

Hafiq Anas, Wee Hong Ong, and Owais Ahmed Malik

Abstract—Classical map-based navigation methods are commonly used for robot navigation, but they often struggle in crowded environments due to the Frozen Robot Problem (FRP). Deep reinforcement learning-based methods address the FRP problem, however, suffer from the issues of generalization and scalability. To overcome these challenges, we propose a method that uses Collision Probability (CP) to help the robot navigate safely through crowds. The inclusion of CP in the observation space gives the robot a sense of the level of danger of the moving crowd. The robot will navigate through the crowd when it appears safe but will take a detour when the crowd is moving aggressively. By focusing on the most dangerous obstacle, the robot will not be confused when the crowd density is high, ensuring scalability of the model. Our approach was developed using deep reinforcement learning (DRL) and trained using the Gazebo simulator in a non-cooperative crowd environment with obstacles moving at randomized speeds and directions. We then evaluated our model on four different crowd-behavior scenarios with varying densities of crowds. The results shown that our method achieved a 100% success rate in all test settings. We compared our approach with a current state-of-the-art DRL-based approach, and our approach has performed significantly better. Importantly, our method is highly generalizable and requires no fine-tuning after being trained once. We further demonstrated the crowd navigation capability of our model in real-world tests.

I. INTRODUCTION

Autonomous mobile robots are increasingly being deployed in human living spaces to provide services such as serving, delivering, and guiding. In these situations, robots must navigate crowded environments with moving humans at varying speeds. This is known as crowd navigation, or social navigation in some cases, where the objective is to navigate between two arbitrary locations in a dynamic environment with many people [1].

The classical navigation approach of using global and local planners has been proven effective for complex environments with both static and dynamic obstacles. A global planner determines the slow and long-term path trajectory to the goal location that the robot should follow, while a local planner determines the fast and short-term path trajectory to avoid obstacles. Popular local planner approaches such as Artificial Potential Fields [2] and Dynamic-Window Approaches [3] made use of an internal map that stores rich environmental information including the position of static obstacles such as walls and dynamic obstacles such as humans. However, these approaches rely heavily on map information which often causes the Frozen Robot Problem (FRP) [4] in crowded

environments, where the robot becomes stuck and unable to move in the presence of dynamic obstacles. To address the limitations of classical planning approaches in crowded environments, recent research works have focused on deep reinforcement learning (DRL) methods. In DRL-based methods, the navigation control strategy is learned by optimizing the parameters that map sensor inputs to velocity commands when the robot is interacting with the environment without the need of a map. Many recent DRL-based works are mapless and have empirical evidence that demonstrates the capability of DRL-based navigation with 2D laser scans for crowd navigation. By removing the reliance on maps, DRL-based methods can help mitigate the FRP problem. DRL-based approaches are however prone to the problem of performing poorly in new unseen scenarios, i.e. the generalization issue. Autonomous mobile robots currently deployed in real-world applications remain dependent on cooperation from the crowd (humans) during navigation.

In this paper, we propose a DRL-based approach using 2D laser scans to remove map reliance to solve the FRP problem in crowd navigation as well as improve the generalization and scalability of the learned model. Our approach differs from the classical approach in that it solves both global and local navigation problems collectively by designing the observation space to incorporate relative goal information and risk perception of the moving obstacles in the crowd. We evaluated our approach in different crowd behavior settings with varying numbers of obstacles at different speeds to evaluate its generalization capability, and compared our results with the results of a recent state-of-the-art DRL-based approach [5] under the same set of test conditions. The main contributions of this work are the ideas of including the risk perception in the observation space to ensure generalization, and focusing on the most dangerous obstacle to ensure scalability of the model. We have also verified the ideas through successful implementations in both simulation and real-world settings.

II. RELATED WORKS

A. Frozen Robot Problem

The Frozen Robot Problem [4] is a prevalent issue in crowd navigation using map-based approaches from classical methods [2][3]. These methods rely heavily on the accuracy of the map to compute a collision-free trajectory based on the relative position of detected obstacles from the robot's velocity and position. However, the introduction of moving obstacles in crowded environments constantly alters the perceived free space on the map, requiring the

planner to frequently replan new navigation routes. As crowd density increases, the available free space to generate a safe navigation path decreases, leading to the robot getting stuck in an endless loop of replanning and causing the Frozen Robot Problem.

B. DRL-based Mapless Navigation with 2D Laser Scans

Deep reinforcement learning (DRL) based mapless approaches in navigation have shown potential in mitigating the Frozen Robot Problem. Looking at the past approaches [5][6][7][8] which are mapless, we have observed that they have used 2D laser scans with different training methods to address different purposes. 2D laser scans have been shown to provide sufficient spatial information to learn useful policies in DRL-based approaches. For example, Tai et al. [6] trained a robot using 10 sparse laser scans and the relative target goal position in a simulated static environment. The trained model was then tested in the real world and demonstrated robustness in crowd-less indoor navigation. They compared their mapless approach with a map-based method called Move Base and showed that their approach was collision-free. Similarly, Zhelo et al. [7] used 72 laser scans and the relative distance and orientation of the target goal position to train their robot in a static environment with similar observation states. They used the Intrinsic Curiosity Model (ICM) [9] to model intrinsic rewards from prediction loss and encourage the robot to find new states for better exploration. The addition of ICM significantly improved navigation success rates and generalization performance in different crowd-less environments. While these works demonstrated the potential of DRL-based mapless navigation, they were developed only for crowd-less environments.

To address the crowd navigation problem, the CrowdMove implementation [8] was proposed. CrowdMove was trained and tested in multiple dynamic environments using commonly used observation states, such as the robot's own velocity and relative target goal position. Unlike the sparse laser scans used in previous studies, CrowdMove used 512 laser scans. The authors concluded that their robot was able to avoid moving obstacles in real-world tests and that their trained model could be generalized to different environment settings unseen during training. We note that their approach relied on providing sufficient variation in the training data of multiple dynamic environments to improve generalization.

Lastly, Jin et al. [5] proposed that a robot moving in a crowded environment should have human-awareness competencies. Therefore, they implemented this through their reward setup by incorporating two conditions: ego-safety and social-safety violations. Using this reward setting, they trained their robot in one crowded environment and tested it in four different crowd behavior environments with varying number of moving obstacles. They achieved significant performance improvement over the then state-of-the-art DRL-based crowd navigation method, CADRL [10]. They achieved success rates between 60% to 100% in various test environments. In their real-world tests, they verified that their robot can safely navigate to a goal position without a

collision. To the best of our knowledge, their work is the current state-of-the-art in crowd navigation using 2D laser scans.

C. Our Work

Our proposed method builds upon the techniques used in the DRL-based methods discussed above, with an addition of perceived risk in the observation states and prioritizing the most dangerous obstacle within a crowd. To determine which obstacle to prioritize, we compute the collision probability of all tracked moving obstacles within the robot's field of view (FOV) and focus on the obstacle with the highest probability of collision. Unlike the method used by Jin et al. [5], we incorporate perceived risk or human-awareness into the observation states, which allows the robot to perceive potential risk during testing or deployment, without the need for extensive training. Jin et al. [5] used ego and social scores in their reward function to model human-awareness, but this approach is limited by the lack of access to such information during deployment. In this sense, their model will require large amount of training to infer the perceived risk from the typical observation states in different scenarios. In addition, we have tested our robot at a significantly higher relative speed of the obstacles to the speed of the robot than in [5].

III. APPROACH

A. Problem Formation

Our approach models the environment as a Partially-Observable Markov Decision Process (POMDP), which is a standard framework for decision-making under uncertainty. Formally, a POMDP is defined by six components: S is the state space, A is the action space, P is the transition probability that specifies the probability of transitioning from one state to another when an action is taken, R is the reward function, Ω is the observation space, and O is the observation probability that specifies the probability of observing a certain observation when the environment is in a certain state. In reinforcement learning, the objective is to learn a policy $\pi(a|s)$, which is a mapping from states to actions that maximizes the expected sum of discounted rewards over time.

Fig. 1 shows the overview of our deep reinforcement learning (DRL) system. The components in the DRL system are described in the following subsections.

1) **Observation space:** The observation space contains input features to learn as well as perform crowd navigation behavior that solves both local and global navigation. To solve the global navigation problem, the information of relative distance to goal (DTG) and orientation (heading to goal, HTG) of the target goal location are used as the goal-related observations o_g . Meanwhile, o_l contains distance information from the 2D laser scan sensor that describe the static environment of the robot and is used to solve the local navigation problem. Given that a crowded environment is associated with moving obstacles, we added agent-related observations o_a and critical obstacle observation o_{co} to the observation space. o_a contains the robot's position ($R_{x,y}$) and

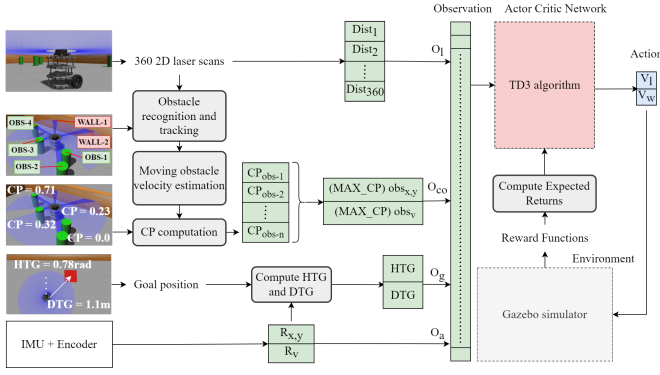


Fig. 1. Deep Reinforcement Learning system structure.

velocity (R_v) estimated from its encoder and inertia sensor. o_{co} describes the position ($obs_{x,y}$) and velocity (obs_v) of the most dangerous moving obstacle (critical obstacle). We define an observation as $o = [o_l, o_g, o_a, o_{co}]$ which describes the partial environment the robot can observe at a given time.

Obstacles tracking was implemented for obstacle velocity estimation and computation of Collision Probability (CP). Using the 2D laser scans o_l , the robot can differentiate between the wall and the moving obstacles, and hence moving obstacles can be tracked. First, the 2D laser scans' values in o_l are converted to cartesian coordinates using the robot's position and orientation. We use Kuhn-Munkres algorithm [11][12] to segment the coordinate values of the scans into N number of groups that correspond to the possible number of obstacles seen by the robot. Then for each group, we compute the gradient of each pair of laser scans' coordinates to determine the object type (wall or obstacle). A scan group is determined to be a wall object if all computed gradients are close to zero. While an obstacle type is confirmed otherwise. Finally, we separate the scans that belong to different object types and use the center scan of each group as the position of the object for tracking, velocity estimation, and CP computation.

We define the Collision Probability (CP) as the sum of two component probabilities: the probability of collision based on the time to collision (P_{c-ttc}) and the probability of collision based on the distance to the obstacle (P_{c-dto}). We argue that the addition of distance to obstacle (dto) information allows the robot to better perceive the collision probability with a moving obstacle in the crowd. For example, a tracked obstacle moving slowly alongside the robot at a close distance can still pose a reasonable amount of danger while a tracked obstacle moving fast toward the robot from a far distance is less dangerous. Therefore, a balance between the two CP components is made as given in (1).

$$CP = \alpha \cdot P_{c-ttc} + (1 - \alpha) \cdot P_{c-dto} \quad (1)$$

where $\alpha \in [0, 1]$ is the parameter that decides the weight of collision probabilities P_{c-dto} and P_{c-ttc} . We have set $\alpha = 0.5$ in the experiments reported in this paper.

The calculation of collision probabilities uses the Collision

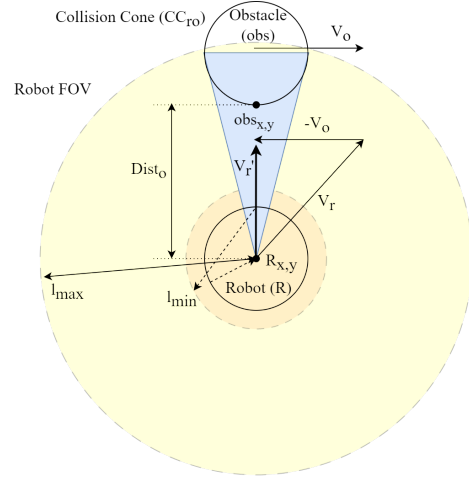


Fig. 2. The Collision Cone and related information.

Cone (CC) concept in [13][14]. Fig. 2 shows an illustration of the CC and the related information that are used to estimate the two components of CP. P_{c-ttc} is computed based on time to collision as defined in (2). P_{c-dto} is computed based on relative distance to obstacle and defined in (3).

$$P_{c-ttc} = \begin{cases} \min(1, \frac{0.15}{t}), & \text{if } V_r' \in CC_{ro} \\ 0 & \text{otherwise} \end{cases} \quad (2)$$

where t is the time-to-collision (TTC) when the relative velocity V_r' between the robot and the obstacle lies within the Collision Cone CC_{ro} . $V_r' = V_r - V_o$ is the resultant velocity between the robot velocity V_r and obstacle velocity V_o . $t = Dist_o / V_r'$ is the time to collision. CC_{ro} is the collision cone area between the robot and obstacle. Finally, 0.15 corresponds to the timestep value of the robot in seconds for executing its velocity commands.

$$P_{c-dto} = \begin{cases} \frac{l_{max} - Dist_o}{l_{max} - l_{min}}, & \text{if } Dist_o < l_{max} \\ 0 & \text{otherwise} \end{cases} \quad (3)$$

where l_{max} and l_{min} are the maximum and minimum range of the laser scan respectively. $Dist_o$ is the distance from the robot to the obstacle of interest.

CP is computed for each obstacle in the list of tracked obstacles and the position ($obs_{x,y}$) and velocity ($obs_v = V_o$) of the obstacle with the highest CP is included in the observation space as o_{co} . This obstacle is seen as most probable to be in collision with the robot.

2) **Action space:** An action is defined as $a = [V_l, V_w]$ which is sampled from a stochastic policy π given observation o : $a \sim \pi(a | o)$ where V_l is the linear velocity within the range $[0, 0.22] \text{ m.s}^{-1}$ and V_w is the angular velocity within the range $[-2.0, 2.0] \text{ rad.s}^{-1}$.

3) **Reward functions:** Our objective is to ensure collision-free navigation in a crowded environment. During training, the robot accumulates rewards and penalties from the Gazebo simulator. Overall, the reward function consists of the following terms:

$$R = R_{step} + R_{dtg} + R_{htg} + R_{goal} + R_{col} \quad (4)$$

$R_{step} = -2$ is the negative reward given to the robot for every step and serves to encourage the robot to avoid abusing the R_{dtg} and R_{htg} rewards by oscillating around the goal location without reaching it.

$$R_{dtg} = \begin{cases} +1, & \text{if } d(r, g)_t < d(r, g)_{t-1} \\ 0 & \text{otherwise} \end{cases} \quad (5)$$

R_{dtg} is the positive reward given to the robot whenever the distance from the robot to the target goal location $d(r, g)$ has reduced between the current and previous timestep.

$$R_{htg} = \begin{cases} +1, & \text{if } \theta(r, g)_t < \theta(r, g)_{t-1} \\ 0 & \text{otherwise} \end{cases} \quad (6)$$

Similarly, R_{htg} is the positive reward given whenever the relative heading $\theta(r, g)$ has decreased.

$R_{goal} = +200$ is the large positive reward given to the robot when it reaches the target goal location. If a collision occurs, a penalty $R_{col} = -200$ is given instead.

B. Deep Reinforcement Learning

Twin Delayed Deep Policy Gradient (TD3) [15] algorithm was chosen over Deep Deterministic Policy Gradient (DDPG) [16] because it solves the overestimation bias problems of DDPG by having two dueling critic networks instead of one. The default parameters were used for TD3.

1) **Model training:** The robot was trained in the Gazebo simulator using Robotis TurtleBot3 Burger platform that is equipped with a LDS-01 360-degree 2D laser scanner and XL430-W250 encoder motors. The resolution of the laser scanner is 360 with a minimum and maximum range set to 0.105m and 0.6m respectively. The training process was done once in a 2m x 2m space with walls and 14 moving obstacles moving at a random speed of up to 0.2m/s in random directions. The moving obstacles were non-cooperative so they will ignore the robot's presence and can collide with the robot. The model was trained for 3000 episodes with the stopping criteria of collision with an obstacle or having reached the goal.

2) **Model testing:** The robot was trained in one simulation setting using TD3 and tested in different crowd behavior settings. The crowd was non-cooperating.

IV. EVALUATION

A. Frozen Robot Problem

We compared the performance of the robot running our model and running the ROS Navigation stack under the same test environments in the Gazebo simulator.

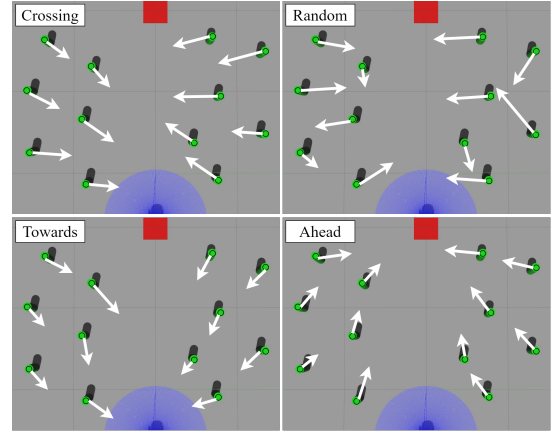


Fig. 3. The four crowd behavior settings with 12 obstacles in Gazebo. **Crossing:** The robot has to navigate through the crowd moving in the crossing directions. **Towards:** The crowd is moving toward the general direction of the robot. **Ahead:** The crowd is moving ahead of the robot. **Random:** The crowd is moving in random directions.

B. Crowd Navigation

We evaluated our robot in different crowd behavior environments similar to [5]: crossing, towards, ahead and random. For each crowd behavior, the model was tested with three different crowd densities of four, eight and twelve obstacles, except the random crowd behavior was only tested with twelve moving obstacles. This gave a total of ten test settings. For each crowd behavior setting, we computed the average of each metric over 10 separate runs. Fig. 3 shows the four crowd behavior settings with 12 moving obstacles.

To quantify performance, we used the same evaluation metrics from Jin et al.'s [5] work: success rate (%), arriving time (s), ego score (0-100) and social score (0-100). Let k be the number of ego-safety violation steps, and N be the total steps to reach the goal, then $Ego_Score = (1 - k/N) * 100$. Let m be the number of social-safety violation steps, then $Social_Score = (1 - m/N) * 100$.

An ego-safety violation is determined when an obstacle comes close to the robot within the ego radius of the robot. We have set the ego radius according to the ratio of the largest width of their Jackal robot to the largest width of our Turtlebot3. Their robot's ego radius was 0.4m for the robot width of 0.508m giving a ratio of 0.787. With the same ratio, we obtained an ego radius of 0.14m for our robot's largest width of 0.178m. In [5], they have determined the social-safety violation when two rectangular spaces computed from the speed of the robot and the speed of an obstacle intersect. The rectangular spaces are similar to the concept of Collision Cone in our case. For the social-safety violation, we have used the CP to determine if our robot is in a collision trajectory course with an obstacle when the CP value is greater than 0.4.

For comparison purposes, we have determined by watching Jin et al.'s demonstration video [5] that their obstacles were moving about 5 times slower than the max speed of their robot (1.5m/s) by observing the time taken for their robot and obstacles to traverse 1 square space (1m)

in Gazebo. In our case, we performed two separate tests with slow-moving and fast-moving obstacles. The slow-moving obstacles moved at a speed that is 2 times slower (0.1m/s) than our robot's max speed (0.22m/s). The fast-moving obstacles moved at a speed (0.2m/s) that is nearly the same as our robot's speed. We believe that in real-world situations, the crowd would be moving at a speed close to each other.

We deployed our model on Turtlebot3 and conducted real-world tests. The robot was tested in the four crowd behaviors with four obstacles. We have used mobile robots with similar size to the Turtlebot3 as the moving obstacles. The moving obstacles were manually teleoperated by humans. It was difficult to teleoperate the obstacles when there are many of them, hence we have limited the real-world tests to four obstacles.

V. RESULTS AND DISCUSSION

A. Frozen Robot Problem

We observed that our approach did not exhibit FRP during training and testing as the robot could navigate smoothly to the goal positions without getting stuck in the crowd. In comparison, frequent freezing was observed when using the ROS Navigation stack in the crowded environments. This was because the perception of free space on the map was continuously changing due to the existence of dense moving obstacles resulting in frequent replanning in map-based navigation. This performance comparison can be seen in the supplementary video of this paper. We can see that the ROS Navigation Stack froze after encountering many moving obstacles, which had cluttered the free space in the map.

B. Crowd Navigation

Fig. 4 shows the evaluation results of our method in comparison to the results Jin et al. [5]. Our robot was able to avoid obstacles with smooth and fast maneuver that resulted in 100% Success Rates (SR) in all test environments. Jin et al.'s [5] success rates were between 60% to 100% with only 10 out of 20 tests achieved 100% success rate.

Our robot took a longer time to reach the goal when the crowd was more dangerous. The arrival times for the test environments with fast moving obstacles (more dangerous) were in general longer than with slow moving obstacles. Likewise, higher crowd density (more dangerous) resulted in longer arrival time. Exceptions were seen in the ahead crowd behavior, where the arrival times with fast moving obstacles ahead were shorter than with slow moving obstacles. The fast moving obstacles were traveling at a speed close to the speed of the robot. In this case, when the obstacles were moving fast ahead of the robot, there was very little chance of the robot being confronted by the obstacles. The ahead environments were quite safe. Consequently, there were very few safety violations as seen from the high ego and social scores in the results of ahead crowd behavior in Fig. 4. While the arrival times of our robot were longer than the results of [5], we note that their robot was traveling at a speed (1.5m/s) about 7 times faster than our robot (0.22m/s).

Taking into account the speed difference, our approach has performed relatively faster and with higher success rate than the approach of [5].

In addition, we have observed an interesting policy learned by our model. In cases where there were too dense obstacles in the way of the robot, the robot would take a detour and avoid the crowd cluster to reach the goal. However, in most cases, the robot navigated through the crowd. Fig. 5 illustrates the robot's behaviors during navigation. Ego-safety and social-safety violations do not necessary result in collisions. They are measures of how risky the robot was navigating in the crowd. Given that in cases where the ego and social scores were low and the robot was able to successfully navigate through the crowd, it demonstrated that our robot was daring in taking a higher risk to reach the goal faster.

Finally, in real-world tests, we observed similar crowd navigation capability as in the simulation. The robot could navigate around the other moving robots to reach the goal in all the four test cases. However, the physical robot could not move smoothly at the velocities setting used in the simulation. The supplementary video shows the performance of the robot in real-world tests.

C. Ablation Study

To investigate the effect of the Collision Probability (CP) (1) and its two components, we trained the model with two variations: one without P_{c-dto} (distance to obstacle CP) component (Model-CP-ttc), and one without CP completely (Model-no-CP). The results are shown in bottom two rows in Fig. 4.

As anticipated the Model-no-CP achieved a lower success rate and was four times slower in arrival time on average than the model with complete risk perception (full CP). During the tests, the robot was observed to avoid obstacles altogether by trying to detour. Without CP, the model was not able to estimate collision risk, so it learned that the best way to avoid collision was by avoiding the obstacles completely. Surprisingly, the Model-CP-ttc could only achieve 100% success rate in 2 out of 10 test conditions. The success rate was lower than the Model-no-CP. At first sight, it may seem that CP was not helpful. However, by observing the robot, we noticed that the robot was attempting to traverse through the crowd but collided with the obstacles when it was too close to an obstacle. This resulted in a lower success rate, however with a significantly faster arrival time than the Model-no-CP. The P_{c-ttc} (time to collision CP) alone underestimated the danger level of the moving obstacles and was insufficient to perceive the risk during crowd navigation. This caused the robot to be in a situation where it found itself unable to avoid a collision which caused the lower average success rate, especially in higher-density crowd tests (obstacle-12, ahead-12). The addition of P_{c-dto} (distance to obstacle CP) has improved the risk estimation as shown in the superior performance of the model with full CP (3rd and 4th rows) with both slow and fast moving obstacles.

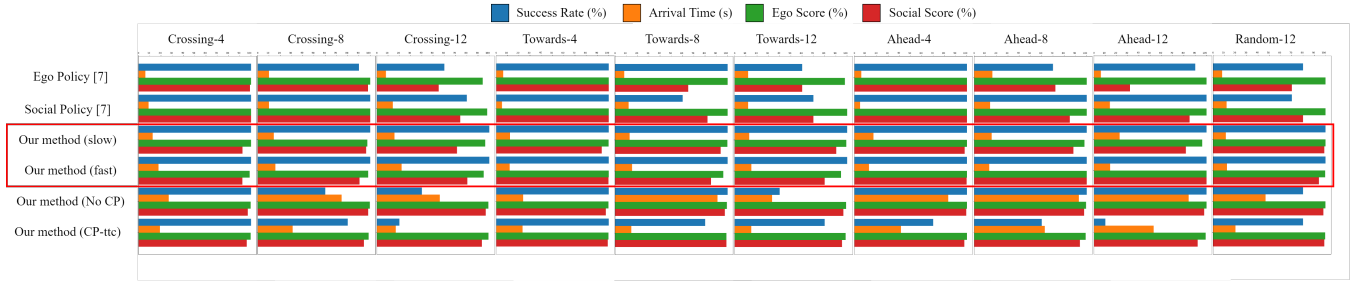


Fig. 4. Comparison between our approach and Jin et al.'s results [5]. Our method was tested with slow and fast moving obstacles. The label of the crowd behavior settings follows the pattern of "behavior-obstacles", e.g. crossing-4 is the test environment with crossing crowd behavior and 4 moving obstacles. The bottom two rows are results of ablation study.

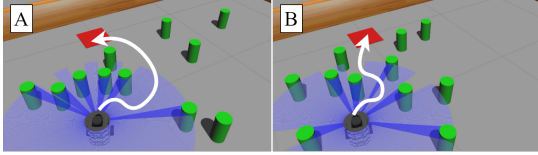


Fig. 5. Robot crowd navigation strategies. **A**: Detour around the obstacles to reach the goal. **B**: Move in between obstacles to reach the goal.

VI. CONCLUSIONS

We have developed a navigation approach for mobile robots using 2D laser scans to improve their performance in crowded environments. Our experiments have shown that our deep reinforcement learning-based mapless approach is effective in circumventing the Frozen Robot Problem (FRP) in comparison to the ROS Navigation Stack when navigating in a crowded environment. In addition, we have shown that the inclusion of the Collision Probability of the most dangerous moving obstacle to the observation space has achieved outstanding performance in crowd navigation, and outperformed the state-of-the-art approach of Jin et al. [5]. Our model was trained in one crowd environment setting and tested on 10 different crowd environment settings. We achieved 100% success rate in all the 10 environment settings including the settings in which the obstacles were moving as fast as the robot. We observed that our model has learned an interesting crowd navigation policy to use different navigation strategies depending on the perceived risk level. Besides the superior performance in the simulated environment, we have also demonstrated the crowd navigation capability of our model in real-world tests. The robot has shown promising performance although not as dexterous as in the simulation. We plan to expand the real-world tests and improve the real-world performance in our future work. We will also investigate further ways to incorporate perceived risk or human-awareness in our crowd navigation approach.

The source code and video demonstration of this work are made publicly available on GitHub [17].

REFERENCES

- [1] K. Zhu and T. Zhang, "Deep reinforcement learning based mobile robot navigation: A review," *Tsinghua Science and Technology*, vol. 26, no. 5, pp. 674–691, 2021.
- [2] F. Arambula Cosío and M. Padilla Castañeda, "Autonomous robot navigation using adaptive potential fields," *Mathematical and Computer Modelling*, vol. 40, no. 9, pp. 1141–1156, 2004.
- [3] D. Fox, W. Burgard, and S. Thrun, "The dynamic window approach to collision avoidance," *IEEE Robotics & Automation Magazine*, vol. 4, no. 1, pp. 23–33, 1997.
- [4] P. Trautman and A. Krause, "Unfreezing the robot: Navigation in dense, interacting crowds," in *2010 IEEE/RSJ International Conference on Intelligent Robots and Systems*, 2010, pp. 797–803.
- [5] J. Jin, N. M. Nguyen, N. Sakib, D. Graves, H. Yao, and M. Jagersand, "Mapless navigation among dynamics with social-safety-awareness: a reinforcement learning approach from 2d laser scans," in *2020 IEEE International Conference on Robotics and Automation (ICRA)*, 2020, pp. 6979–6985.
- [6] L. Tai, G. Paolo, and M. Liu, "Virtual-to-real deep reinforcement learning: Continuous control of mobile robots for mapless navigation," in *2017 IEEE/RSJ International Conference on Intelligent Robots and Systems (IROS)*, 2017, pp. 31–36.
- [7] O. Zhelo, J. Zhang, L. Tai, M. Liu, and W. Burgard, "Curiosity-driven exploration for mapless navigation with deep reinforcement learning," in *ICRA 2018 Workshop on Machine Learning in Planning and Control of Robot Motion*, May 2018.
- [8] P. Long, T. Fan, X. Liao, W. Liu, H. Zhang, and J. Pan, "Towards optimally decentralized multi-robot collision avoidance via deep reinforcement learning," in *2018 IEEE International Conference on Robotics and Automation (ICRA)*, 2018, pp. 6252–6259.
- [9] D. Pathak, P. Agrawal, A. A. Efros, and T. Darrell, "Curiosity-driven exploration by self-supervised prediction," in *Proceedings of the 34th International Conference on Machine Learning*, vol. 70. PMLR, 2017, pp. 2778–2787.
- [10] Y. F. Chen, M. Liu, M. Everett, and J. P. How, "Decentralized non-communicating multiagent collision avoidance with deep reinforcement learning," in *2017 IEEE International Conference on Robotics and Automation (ICRA)*, 2017, pp. 285–292.
- [11] H. W. Kuhn, "The hungarian method for the assignment problem," *Naval research logistics quarterly*, vol. 2, no. 1-2, pp. 83–97, 1955.
- [12] J. Munkres, "Algorithms for the assignment and transportation problems," *Journal of the society for industrial and applied mathematics*, vol. 5, no. 1, pp. 32–38, 1957.
- [13] L. Sun, J. Zhai, and W. Qin, "Crowd navigation in an unknown and dynamic environment based on deep reinforcement learning," *IEEE Access*, vol. 7, pp. 109 544–109 554, 2019.
- [14] P. Fiorini and Z. Shiller, "Motion planning in dynamic environments using velocity obstacles," *The international journal of robotics research*, vol. 17, no. 7, pp. 760–772, 1998.
- [15] S. Fujimoto, H. Hoof, and D. Meger, "Addressing function approximation error in actor-critic methods," in *International conference on machine learning*. PMLR, 2018, pp. 1587–1596.
- [16] T. P. Lillicrap, J. J. Hunt, A. Pritzel, N. Heess, T. Erez, Y. Tassa, D. Silver, and D. Wierstra, "Continuous control with deep reinforcement learning," in *4th International Conference on Learning Representations, ICLR 2016*, 2016.
- [17] H. Anas. Deep reinforcement learning based crowd navigation with perceived risk of the moving crowd for mobile robots. [Online]. Available: <https://github.com/ailabspac/drl-based-mapless-crowd-navigation-with-perceived-risk>